Discovery of allodiploid hybrid species *Aspergillus latus* in Japan

Saho Shibata[1], Momotaka Uchida[1], Sayaka Ban[1], Katsuhiko Kamei[1], Akira Watanabe[1], Takashi Yaguchi[1], Vit Hubka[2,3], Hiroki Takahashi[1,4,5]

[1]Medical Mycology Research Center, Chiba University, 1-8-1 Inohana, Chuo-ku, Chiba 260-8673, Japan

[2]Laboratory of Fungal Genetics and Metabolism, Institute of Microbiology, Czech Academy of Sciences, Vídeňská 1083, 142 00 Prague 4, Czech Republic

[3]Department of Botany, Faculty of Science, Charles University, Benátská 2, 128 00 Prague 2, Czech Republic

[4]Molecular Chirality Research Center, Chiba University, 1-33 Yayoi-cho, Inage-ku, Chiba 263-8522, Japan.

[5]Plant Molecular Science Center, Chiba University, 1-8-1 Inohana, Chuo-ku, Chiba 260-8675, Japan.

Address for correspondence: Hiroki Takahashi

E-mail: hiroki.takahashi@chiba-u.jp

ORCID

S. Shibata: 0000-0003-2336-6948

M. Uchida: 0000-0001-5642-1435

S. Ban: 0000-0003-3442-308X

K. Kamei: 0000-0002-6067-9049

A. Watanabe: 0000-0002-3057-2937

T. Yaguchi: 0000-0002-9697-8470

V. Hubka: 0000-0003-4583-6496

H. Takahashi: 0000-0001-5627-1035

Abstract

Allodiploid hybrid species, *Aspergillus latus*, belonging to section *Nidulantes*, is a hybrid of *A. spinulosporus* and unknown species closely related to *A. quadrilineatus* and *A. subltus*. This hybrid has often been misidentified as the species in section *Nidulantes*, such as *A. nidulans*, *A. spinulosporus*, *A. sublatus*, or other cryptic species. *A. latus* has not been reported in Japan as well as Asia so far. In this study, we screened 23 clinical strains identified as *A. spinulosporus* isolated in Japan from 2012 to 2023 and found seven *A. latus* strains. To characterize the *A. latus* strains, we conducted comprehensive phenotyping including morphological observation, whole genome sequences and phylogenetic analysis based on calmodulin (*CaM*) gene. In addition, we conducted antifungal susceptibility testing for *A. latus* strains. As a result, the morphological characters of *A. latus* were more similar to those of *A. spinulosporus* compared to *A. sublatus*. However, the ascospore of *A. latus* differed from that of *A. spinulosporus*. *A. latus* phylogenetically clustered with *A. spinulosporus* and *A. sublatus*. Furthermore, *A. latus* strains showed reduced susceptibility to caspofungin and amphotericin B compared to *A. spinulosporus*, while they were susceptible to azoles. Our results suggest that *A. latus* has been a causative pathogen of aspergillosis in Japan since 2013.

Keywords: *Aspergillus latus, Aspergillus spinulosporus*, *Aspergillus sublatus*, section *Nidulantes*, aspergillosis

Introduction

Aspergillus species are the causal agents for aspergillosis, mainly affecting immunocompromised individuals [1, 2]. Although *A. fumigatus* is a main causative agent, other species such as *A. nidulans*, *A. flavus*, *A. niger*, and *A. terreus* also contribute to the disease [3–6]. *Aspergillus nidulans*, a member of the section *Nidulantes* poses a serious threat to immunocompromised patients, especially those with chronic granulomatous disease [3]. Additionally, eleven other species within the section *Nidulantes* have been isolated from patients with invasive aspergillosis [7]. Recently, Steenwyk et al. (2020) through screening of *A. nidulans* strains identified that *A. latus* is an allodiploid hybrid species between *A. spinulosporus* and unknown species closely related to *A. quadrilineatus*, and exhibits higher virulence and minimum inhibitory concentrations to some antifungals than *A. nidulans* [8]. This highlights the importance of accurate species identification to ensure effective treatment, as misidentification could compromise patient care.

Steenwyk et al. (2020 & 2024) reported 30 *A. latus* strains from Belgium, Brazil, France, Germany, Netherlands and Portugal identified as *A. nidulans*, *A. spinulosporus*, or other cryptic species, suggesting that *A. latus* infections are likely underreported [9]. Prospective survey in single center in Japan reported that six *A. nidulans* strains were identified among 107 *Aspergillus* strains [11]. To date, *A. latus* has not been reported in Asia including Japan. However, *A. nidulans*

67 and some cryptic species were isolated from patients in Japan, namely *A. latus* could had also
68 been isolated [10, 11].

69 In this study, we identified seven clinical *A. latus* strains isolated in Japan by screening 23 *A.*
70 *spinulosporus* strains which were collected between 2012 and 2023. To characterize these seven
71 *A. latus* strains isolated in Japan, we performed comprehensive phenotyping including
72 morphological observations, whole genome sequences and phylogenetic analysis based on
73 calmodulin (*CaM*) gene. In addition, we measured the antifungal susceptibility of these strains to
74 six antifungals. Here, we present the first report of *A. latus* being isolated in Japan. Our findings
75 indicate that *A. latus* has been the causative agent of aspergillosis in Japan since 2013.

76

77 **Material and methods**

78 **Strains**

79 *A. latus*, *A. sublatus* and *A. spinulosporus* strains used in this study have been stored and
80 maintained at the Medical Mycology Research Center, Chiba University (IFM strains) in Japan.
81 A total of 23 strains of *A. latus* and *A. spinulosporus* are clinical isolate in Japan, and *A. sublatus*
82 IFM 42029 (= IFM 4553 = CBS 140630) is a type strain collected from soil in Brazil.

83

84 **Genomic DNA extraction**

85 Fungi were incubated on Potato Dextrose Agar (Thermo Fischer Scientific, MA, USA) at
86 30 °C for 7 days to obtain fully mature conidia. The conidia were inoculated in Potato Dextrose
87 Broth (Thermo Fischer Scientific) at 37 °C at 180 rpm for 16 h. Mycelia were washed with H_2O,
88 and genomic DNA was purified with phenol-chloroform extraction and Monarch® Genomic DNA
89 Purification Kit (New England Biolabs, MA, USA) [12, 13]. The DNA concentration and quality
90 were then measured by Qubit Fluorometer (Thermo Fischer Scientific). The extracted DNA were
91 used for cloning of *CaM* gene and whole-genome sequencing.
92
93 **Whole genome sequencing and assembly**
94 Whole-genome 150 bp paired-end (PE) sequencing of four *A. latus* strains, IFM 65030, IFM
95 65233, IFM 65239 and IFM 66778 was performed using Illumina NovaSeq 6000 (Illumina, CA,
96 USA) by Novogene Biotech Co. (Beijing, China). The raw genomic reads were trimmed using
97 fastp v.0.20.1 [14]. The mitochondrial genomes were assembled using GetOrganelle v.1.6.4 [15].
98 To filter the mitochondrial reads, the reads were aligned with the mitochondrial genome using
99 BWA-MEM v.0.7.17-r1188 [16]. The mapped reads were filtered using SAMtools v.1.10 [17] and
100 SeqKit v.0.10.1 [18]. The nuclear genomes were assembled using VelvetOptimiser v.2.2.6 [19].
101 The completeness of draft genomes was evaluated by BUSCO v. 5.2.1 [20] with the database
102 eurotiales_odb10. blastn v.2.15.0+ [21] was used for extracting the sequences of *CaM* of *A. latus*

103 strains by serving the sequence of *A. nidulans* FGSC A4 as query sequence. The genome sizes of

104 *A. latus* strains were estimated using Jellyfish [22] and GenomeScope with 21 k-mers [23].

105

106 **DNA Cloning and Sequencing**

107 The cloning of two *CaM* genes of three strains, IFM 61956, IFM 63852 and IFM 64630, were

108 performed. PCR amplification was performed by Quick Taq® HS DyeMix (TOYOBO, Tokyo,

109 Japan) in a ProFlex™ PCR System (Thermo Fisher Scientific) with a program consisting of an

110 initial denaturing step at 94 °C for 2 min: 35 cycles of denaturation at 94 °C for 30 sec, annealing

111 at 50 °C for 30 sec, and extension at 68 °C for 1 min. The amplicons of *CaM* were obtained by

112 PCR with primer pairs CF1L_SacI (5′-AAAGAGCTCGCCGACTCTTTGACYGARGAR-3′)

113 and CF4_SacI (5′-AAAGAGCTCTTTYTGCATCATRAGYTGGAC-3′). These primers contain

114 the sequence of CF1 and CF4 primers, respectively, from a previous study [24, 25], with the SacI

115 restriction site at the 5′ end. The PCR amplicons were purified by gel extraction with QIAquick

116 Gel Extraction Kit (QIAGEN, Hilden, Germany). The objective gene fragments were cloned into

117 pMK-dGFP vector [26], and introduced into competent cells of *Escherichia coli* DH5α. FastGene

118 Plasmid Mini Kit (Nippon Genetics, Tokyo, Japan) was used to extract the plasmid DNA. The

119 plasmid (ca. 2.0 μL) was used as the templates for the sequencing reaction with a BigDye

120 Terminator v3.1 Cycle Sequencing Kit (Thermo Fisher Scientific) along with PtrpC-Rev (5′-

121 AAATGCTCCTTCAATATCATCTTCTGTCGA-3′) and M13R (5′-
122 CAGGAAACAGCTATGAC-3′) primers [27], following the manufacturer's instructions. Ethanol
123 precipitation was used to remove excess fluorescent dye-terminators from cycle sequencing
124 reactions prior to analysis on an automated sequencer. Sequence was performed with an ABI 3100
125 Genetic Analyzer (Thermo Fisher Scientific).
126
127 **Phylogenetic analysis**
128 The sequences of *CaM* ranging from 438 bp to 824 bp in length were aligned with MAFFT
129 v.7.508 [28, 29]. Aligned sequences were trimmed using trimAl v.1.4.rev15 [30], resulting in 686
130 bp in length. The maximum likelihood tree of *CaM* was constructed using the multithreaded
131 version of RAxML v.8.2.12 [31], the GTRCAT model, and 1,000 bootstrap replicates. The
132 phylogenetic tree was visualized using the FigTree (free download available at
133 http://tree.bio.ed.ac.uk/software/figtree/). A total of 112 taxa were included in our tree
134 (Supplementary Table S1).
135
136 **Morphological observations**
137 *A. latus* IFM 65329 was used for microscopic and macroscopic observation. The colony
138 character of the other six strains of *A. latus*, *A. sublatus* IFM 42029^{T} (= IFM 4553^{T}) and *A.*

139 *spinulosporus* IFM 66771 were observed. The observations of macroscopic characters were
140 curried on the agar media, i.e., Czapek yeast autolysate agar (CYA, Czapeck Dox Agar, Duchefa
141 Biochemie, Haarlem, Netherlands and Difco™ Yeast Extract, Thermo Fischer Scientific), oatmeal
142 agar (OA, Sigma Aldrich, MO, USA) and malt extract agar (MEA, Thermo Fischer Scientific)
143 with trace elements (0.1 g $ZnSO_4 \cdot 7H_2O$ and 0.5 g $CuSO_4 \cdot 5H_2O$ in 100 mL distilled water) at 25
144 or 37 °C for 7 days. Microscopic observations of conidia and conidiophores were made from 1
145 week old colonies on MEA. Ascomata and ascospores were observed from 8-week-old colonies
146 on OA. A light microscope (Nikon ECLIPSE Ni, Tokyo, Japan and Swift Optical Instruments S7-
147 TP520, TX, USA) was used to examine morphological characters including the size and shape of
148 ascomata, ascospores, conidiophores and conidia. These were mounted in a drop of water on glass
149 slides. The slide preparations were examined and photographed using a digital camera (Nikon
150 DS-Fi3, Japan). Approximately 30 structures were randomly chosen, and their length and width
151 were measured using 'ImageJ' software (free download available at http://rsbweb.nih.gov/ij/).
152

153 **Antifungal susceptibility testing**

154 Minimum inhibitory concentration (MIC) tests for amphotericin B (AMPH-B), itraconazole
155 (ITCZ), voriconazole (VRCZ), miconazole (MCZ), micafungin (MCFG), and caspofungin
156 (CPFG), were performed using the dried plate for antifungal susceptibility testing of yeasts

157 method (Eiken Chemicals, Tokyo, Japan). The method follows the Clinical and Laboratory
158 Standards Institute M38-E2 with slight modifications [32–34].
159
160 **Results**
161 **Screening and identification of *A. latus***
162 To identify the presence of allodiploid hybrid strains of *A. latus*, we sequenced the *CaM* genes
163 of 23 *A. spinulosporus* strains. Sequences with double peaks were observed in seven strains. The
164 sequences of two copies of *CaM* were determined in all seven strains by either cloning or whole-
165 genome sequencing (Table 1). These strains were isolated from the patients between 2013 and
166 2022. The ages of the patients ranged from 13 to 79 years. The patients were diagnosed with
167 invasive pulmonary aspergillosis (IFM 63852 and IFM 66778) and chronic pulmonary
168 aspergillosis (IFM 65233 and IFM 65329), the other patients were not diagnosed with
169 aspergillosis (IFM 61956, IFM 64360, and IFM 65030). However, the patients were diagnosed
170 with other diseases such as leukemia. Therefore, we could not conclude that *A. latus* is a primary
171 cause of death.
172 Draft genomes for four *A. latus* strains (IFM 65030, IFM 65233, IFM 65239 and IFM 66778)
173 were generated, with assembled genome sizes ranging from 62.1 Mb to 63.2 Mb, aligning with

174 the typical genome sizes of *A. latus* (previous study showed average genome size 69.09 ± 5.68

175 Mb [8]) (Supplementary Table S2).

176

177 **Phylogenetic analysis**

178 We conducted a phylogenetic analysis to characterize the position of seven Japanese *A. latus*

179 strains. One copy of *CaM* gene sequence clustered with the sequences of *A. spinulosporus*, while

180 the other copy clustered with *A. sublatus* (Fig. 1). The *CaM* sequence of *A. latus* differed from

181 that of *A. sublatus* in length by 1 bp, that of *A. quadrilineatus* in length by 6 bp, but the *CaM*

182 sequence of *A. latus* harbors no specific substitution compared to *A. sublatus*, *A. quadrilineatus*

183 and *A. spinulosporus.*

184

185 **Morphological observations**

186 The colony morphologies of *A. latus* varied among strains (Fig. 2, Supplementary Fig. 1). On

187 MEA, the growth was slower compared to that of *A. sublatus* and *A. spinulosporus* (Fig. 2B,

188 Supplementary Fig. 1B, E, H, K, N, Q, T, W). In terms of colony appearance, *A. latus* was more

189 similar to *A. spinulosporus* than to *A. sublatus*, as its colonies were covered with green conidia

190 on OA and sometimes on CYA (Table 2 and Supplementary Fig. 1C, F, I, L, O, R, X). The

191 microscopic of *A. latus* also closely resembled those of the other two species but ascospores of *A.*

192 *spinulosporus* are echinulated (Table 2) [35, 36].

193

194 **Antifungal susceptibility testing**

195 Antifungal susceptibility testing was conducted on seven *A. latus*, one *A. sublatus*, and three

196 *A. spinulosporus* strains (Table 3). Reduced susceptibility to CPFG was observed in all tested

197 strains, geometric mean MICs of 7.2 for *A. latus*, 16 for *A. sublatus*, and 5.0 for *A. spinulosporus*.

198 Reduced susceptibility to AMPH-B was noted in *A. latus* and *A. sublatus*, while *A. spinulosporus*

199 strains displayed low MICs, with geometric mean MICs of 4.4, 4.0, and 0.7, respectively.

200 *Aspergillus latus* strains displayed low MICs to MCFG, whereas MICs of *A. sublatus*, and *A.*

201 *spinulosporus* were elevated. Susceptibility to VRCZ and MCZ varied: reduced susceptibility to

202 VRCZ was observed in *A. latus* IFM 66778 strain (MIC 2.0), and reduced susceptibility to MCZ

203 was noted in *A. latus* strains IFM 61956 and IFM 65329 (MIC 2.0), as well as *A. sublatus*. All

204 tested strains were susceptible to ITCZ.

205

206 **Discussion**

207 Here, we report the allodiploid hybrid *A. latus* strains isolated in Japan. Although 30 strains

208 have been found worldwide [8, 9], *A. latus* has not been reported in Japan as well as Asia. By

209 screening 23 *A. spinulosporus* strains, we found seven clinical *A. latus* strains (30.4%). *A. latus*
210 IFM 61956 was isolated in 2013, suggesting that this species might be more prevalent in the
211 country. The pathogenicity of *A. latus* was shown to be comparable to that of *A. spinulosporus*
212 and *A. nidulans* [8, 9]. In this study, the pathogenicity of *A. latus* was unclear, because *A. latus*
213 strains could be colonized in most cases (Table 1). However, ongoing monitoring is necessary, as
214 changes in pathogenicity or resistance profiles could impact treatment strategies in the future.

215 We conducted a phylogenetic analysis of *A. latus* (Fig. 1) with results indicating that it is
216 derived from a hybridization between *A. spinulosporus* and a species related to *A. sublatus* and *A.*
217 *quadrilineatus*. Morphological characters of seven *A. latus* strains, such as colony color and
218 growth on MEA, were most stable among strains (Fig. 2B, Table 2, and Supplementary Fig. 1B,
219 E, H, K, N, Q). The differences between *A. latus*, *A. spinulosporus* and *A. sublatus*, however, were
220 slight, and given the variability observed in previous studies, species identification relying on
221 these traits may be challenging (Supplementary Fig. 1) [9].

222 In terms of antifungal susceptibility, strains of *A. latus* found in Japan demonstrated increased
223 susceptibility to ITCZ compared to overseas strains [8], while showing reduced susceptibility to
224 CPFG, aligning with the previous research [8, 9] (Table 3). It has been reported that *A.*
225 *spinulosporus* exhibits reduced susceptibility to CPFG compared to *A. nidulans* and other
226 clinically relevant species in section *Nidulantes* [8, 37]. In this study, we confirmed that *A.*

227 *spinulosporus* and *A. sublatus* showed reduced susceptibility to CPFG, suggesting that this
228 characteristic in *A. latus* may be derived from these species. In addition, *A. latus* strains exhibited
229 AMPH-B resistance. Although high AMPH-B MIC values have been reported in other *Aspergillus*
230 species, especially *A. nidulans* and related species [8, 37, 38], the mechanisms underlying the
231 resistance remain poorly understood. Increased catalase production has been implicated in
232 AMPH-B resistance in *A. terreus* [39], suggesting that *A. latus* may produce high level of catalase.
233 In conclusion, our study provides significant insights into the ecology and clinical relevance
234 of *A. latus*, a newly recognized hybrid pathogen and cryptic species of *A. nidulans*. We
235 documented the first occurrence of this pathogen in Japan, demonstrating its prevalence and
236 potential role as a causative agent of aspergillosis since 2013. The comprehensive phenotyping,
237 including morphological and genetic analysis, underscored the diagnostic challenges due to its
238 similarities with *A. spinulosporus* and *A. sublatus*. Moreover, antifungal susceptibility testing
239 revealed reduced susceptibility to certain antifungal agents, highlighting the need for accurate
240 identification to inform effective treatment strategies. Our findings add to the growing body of
241 knowledge about the distribution and pathogenic characteristics of *A. latus* and emphasize the
242 importance of continued surveillance and accurate diagnostics in clinical mycology.
243

244 **Acknowledgements**

We thank Dr Takayuki Arazoe (Tokyo University of Science) for providing us with the pMK-dGFP plasmid. We thank Junko Ito and Emi Shirai for technical assistance with the experiments. We are also grateful to Machiko Zen for assistance with the data analysis.

References

1. Latgé JP. *Aspergillus fumigatus* and aspergillosis. Clin Microbiol Rev. 1999;12:310–50. https://doi.org/10.1128/CMR.12.2.310
2. Sugui JA, Kwon-Chung KJ, Juvvadi PR, Latgé J-P, Steinbach WJ. *Aspergillus fumigatus* and related species. Cold Spring Harb Perspect Med. 2014;5:a019786. https://doi.org/10.1101/cshperspect.a019786
3. Bastos RW, Valero C, Silva LP, Schoen T, Drott M, Brauer V, et al. Functional Characterization of Clinical Isolates of the Opportunistic Fungal Pathogen *Aspergillus nidulans*. mSphere. 2020;5:e00153-20. https://doi.org/10.1128/mSphere.00153-20
4. Paulussen C, Hallsworth JE, Álvarez-Pérez S, Nierman WC, Hamill PG, Blain D, et al. Ecology of aspergillosis: insights into the pathogenic potency of *Aspergillus fumigatus* and some other *Aspergillus* species. Microb Biotechnol. 2017;10:296–322. https://doi.org/10.1111/1751-7915.12367

5. Zakaria A, Osman M, Dabboussi F, Rafei R, Mallat H, Papon N, et al. Recent trends in the epidemiology, diagnosis, treatment, and mechanisms of resistance in clinical *Aspergillus* species: A general review with a special focus on the Middle Eastern and North African region. J Infect Public Health. 2020;13:1–10. https://doi.org/10.1016/j.jiph.2019.08.007

6. Hashimoto A, Hagiwara D, Watanabe A, Yahiro M, Yikelamu A, Yaguchi T, et al. Drug Sensitivity and Resistance Mechanism in *Aspergillus* Section *Nigri* Strains from Japan. Antimicrob Agents Chemother. 2017;61:e02583-16. https://doi.org/10.1128/AAC.02583-16

7. Arastehfar A, Carvalho A, Houbraken J, Lombardi L, Garcia-Rubio R, Jenks JD, et al. *Aspergillus fumigatus* and aspergillosis: From basics to clinics. Stud Mycol. 2021;100:100115. https://doi.org/10.1016/j.simyco.2021.100115

8. Steenwyk JL, Lind AL, Ries LNA, Dos Reis TF, Silva LP, Almeida F, et al. Pathogenic Allodiploid Hybrids of *Aspergillus* Fungi. Curr Biol. 2020;30:2495-2507.e7. https://doi.org/10.1016/j.cub.2020.04.071

9. Steenwyk JL, Knowles S, Bastos RW, Balamurugan C, Rinker D, Mead ME, et al. Evolutionary origin and population diversity of a cryptic hybrid pathogen. Nat Commun. 2024;15:8412. https://doi.org/10.1038/s41467-024-52639-1

10. Tashiro T. Pulmonary Aspergillosis and clinical significance of *Aspergillus* isolation from respiratory samples. J Jap Soc Clin Microbiol. 2009;19:67–75.

11. Toyotome T, Saito S, Koshizaki Y, Komatsu R, Matsuzawa T, Yaguchi T. Prospective survey of *Aspergillus* species isolated from clinical specimens and their antifungal susceptibility: A five-year single-center study in Japan. J Infect Chemother. 2020;26:321–3. https://doi.org/10.1016/j.jiac.2019.09.002

12. Bian C, Kusuya Y, Sklenář F, D'hooge E, Yaguchi T, Ban S, et al. Reducing the number of accepted species in *Aspergillus* series *Nigri*. Stud Mycol. 2022;102:95–132. https://doi.org/10.3114/sim.2022.102.03

13. Kusuya Y, Bian C, Hagiwara D, Ban S, Takahashi H. A novel Zn2-Cys6 transcription factor clcA contributes to copper homeostasis in *Aspergillus fumigatus*. Curr Genet. 2022;68:605–17. https://doi.org/10.1007/s00294-022-01250-2

14. Chen S, Zhou Y, Chen Y, Gu J. fastp: an ultra-fast all-in-one FASTQ preprocessor. Bioinformatics. 2018;34:i884–90. https://doi.org/10.1093/bioinformatics/bty560

15. Jin J-J, Yu W-B, Yang J-B, Song Y, dePamphilis CW, Yi T-S, et al. GetOrganelle: a fast and versatile toolkit for accurate de novo assembly of organelle genomes. Genome Biol. 2020;21:241. https://doi.org/10.1186/s13059-020-02154-5

16. Li H, Durbin R. Fast and accurate short read alignment with Burrows-Wheeler transform. Bioinformatics. 2009;25:1754–60. https://doi.org/10.1093/bioinformatics/btp324

17. Danecek P, Bonfield JK, Liddle J, Marshall J, Ohan V, Pollard MO, et al. Twelve years of SAMtools and BCFtools. Gigascience. 2021;10:giab008. https://doi.org/10.1093/gigascience/giab008

18. Shen W, Le S, Li Y, Hu F. SeqKit: A Cross-Platform and Ultrafast Toolkit for FASTA/Q File Manipulation. PLoS One. 2016;11:e0163962. https://doi.org/10.1371/journal.pone.0163962

19. Zerbino DR, Birney E. Velvet: algorithms for de novo short read assembly using de Bruijn graphs. Genome Res. 2008;18:821–9. https://doi.org/10.1101/gr.074492.107

20. Seppey M, Manni M, Zdobnov EM. BUSCO: Assessing Genome Assembly and Annotation Completeness. Methods Mol Biol. 2019;1962:227–45. https://doi.org/10.1007/978-1-4939-9173-0_14

21. Camacho C, Coulouris G, Avagyan V, Ma N, Papadopoulos J, Bealer K, et al. BLAST+: architecture and applications. BMC Bioinformatics. 2009;10:421. https://doi.org/10.1186/1471-2105-10-421

22. Marçais G, Kingsford C. A fast, lock-free approach for efficient parallel counting of occurrences of k-mers. Bioinformatics. 2011;27:764–70. https://doi.org/10.1093/bioinformatics/btr011

313 23. Vurture GW, Sedlazeck FJ, Nattestad M, Underwood CJ, Fang H, Gurtowski J, et al.
314 GenomeScope: fast reference-free genome profiling from short reads. Bioinformatics.
315 2017;33:2202–4. https://doi.org/10.1093/bioinformatics/btx153
316 24. Peterson SW. Multilocus DNA sequence analysis shows that *Penicillium biourgeianum* is a
317 distinct species closely related to *P. brevicompactum* and *P. olsonii*. Mycol Res.
318 2004;108:434–40. https://doi.org/10.1017/S0953756204009761
319 25. Peterson SW, Vega FE, Posada F, Nagai C. *Penicillium coffeae*, a new endophytic species
320 isolated from a coffee plant and its phylogenetic relationship to *P. fellutanum*, *P. thiersii* and
321 *P. brocae* based on parsimony analysis of multilocus DNA sequences. Mycologia.
322 2005;97:659-66. https://doi.org/10.3852/mycologia.97.3.659
323 26. Arazoe T, Ohsato S, Arie T, Yoneyama K, Kuwata S. Construction of a system for exploring
324 mitotic homologous recombination in the genome of *Pyricularia oryzae*. J Gen Plant Pathol.
325 2013;79:422–30. https://doi.org/10.1007/s10327-013-0474-2
326 27. Huey B, Hall J. Hypervariable DNA fingerprinting in *Escherichia coli*: minisatellite probe
327 from bacteriophage M13. J Bacteriol. 1989;171:2528–32.
328 https://doi.org/10.1128/jb.171.5.2528-2532.1989

329 28. Katoh K, Misawa K, Kuma K, Miyata T. MAFFT: a novel method for rapid multiple
330 sequence alignment based on fast Fourier transform. Nucleic Acids Res. 2002;30:3059–66.
331 https://doi.org/10.1093/nar/gkf436
332 29. Katoh K, Standley DM. MAFFT multiple sequence alignment software version 7:
333 improvements in performance and usability. Mol Biol Evol. 2013;30:772–80.
334 https://doi.org/10.1093/molbev/mst010
335 30. Capella-Gutiérrez S, Silla-Martínez JM, Gabaldón T. trimAl: a tool for automated alignment
336 trimming in large-scale phylogenetic analyses. Bioinformatics. 2009;25:1972–3.
337 https://doi.org/10.1093/bioinformatics/btp348
338 31. Stamatakis A. RAxML version 8: a tool for phylogenetic analysis and post-analysis of large
339 phylogenies. Bioinformatics. 2014;30:1312–3.
340 https://doi.org/10.1093/bioinformatics/btu033
341 32. Kikuchi K, Watanabe A, Ito J, Oku Y, Wuren T, Taguchi H, et al. Antifungal susceptibility of
342 *Aspergillus fumigatus* clinical isolates collected from various areas in Japan. J Infect
343 Chemother. 2014;20:336–8. https://doi.org/10.1016/j.jiac.2014.01.003
344 33. CLSI. Reference method for broth dilution antifungal susceptibility testing of filamentous
345 fungi. In: CLSI standard M38, 3rd edn. Clinical and Laboratory Standards Institute, Wayne,
346 PA; 2017.

347 34. He X, Kusuya Y, Hagiwara D, Toyotome T, Arai T, Bian C, et al. Genomic diversity of the
348 pathogenic fungus *Aspergillus fumigatus* in Japan reveals the complex genomic basis of
349 azole resistance. Commun Biol. 2024;7:274. https://doi.org/10.1038/s42003-024-05902-6
350 35. Chen AJ, Frisvad JC, Sun BD, Varga J, Kocsubé S, Dijksterhuis J, et al. *Aspergillus* section
351 *Nidulantes* (formerly *Emericella*): Polyphasic taxonomy, chemistry and biology. Stud Mycol.
352 2016;84:1–118. https://doi.org/10.1016/j.simyco.2016.10.001
353 36. Horie Y. New or interesting *Emericella* from herbal drugs. Trans Mycol Soc Japan.
354 1979;20:481–91.
355 37. Tavakoli M, Rivero-Menendez O, Abastabar M, Hedayati MT, Sabino R, Siopi M, et al.
356 Genetic diversity and antifungal susceptibility patterns of *Aspergillus nidulans* complex
357 obtained from clinical and environmental sources. Mycoses. 2020;63:78–88.
358 https://doi.org/10.1111/myc.13019
359 38. Van Der Linden JWM, Warris A, Verweij PE. *Aspergillus* species intrinsically resistant to
360 antifungal agents. Med Mycol. 2011;49 Suppl 1:S82-89.
361 https://doi.org/10.3109/13693786.2010.499916
362 39. Blum G, Perkhofer S, Haas H, Schrettl M, Würzner R, Dierich MP, et al. Potential basis for
363 amphotericin B resistance in *Aspergillus terreus*. Antimicrob Agents Chemother.
364 2008;52:1553–5. https://doi.org/10.1128/AAC.01280-07

Statements & Declarations

Funding

This work was partly supported by JSPS KAKENHI Grant No. 24K19262.

Competing Interests

The authors have no relevant financial or non-financial interests to disclose.

Author Contributions

Saho Shibata, Vit Hubka, and Hiroki Takahashi contributed to the study conception and design. Material preparation, data collection and analysis were performed by Saho Shibata, Momotaka Uchida, Sayaka Ban, Kamei Katsuhiko, Akira Watanabe, Vit Hubka, and Hiroki Takahashi. The draft of the manuscript was written by Saho Shibata, Momotaka Uchida, Takashi Yaguchi, Vit Hubka and Hiroki Takahashi, and all authors commented on the manuscript. All authors read and approved the final manuscript.

Ethical approval

No ethical approval is required

383 **Table 1.** Clinical information of *Aspergillus latus* strains examined in this study

Strain No.	Species name		Isolation year	Disease record	Age	Outcome
	this study	previous identified				
IFM 61956	*A. latus*	*A. spinulosporus*	2013	colon cancer, pneumonia	N/A	dead
IFM 63852	*A. latus*	*A. spinulosporus*	2016	interstitial lung disease, invasive pulmonary aspergillosis	79	dead
IFM 64360	*A. latus*	*A. spinulosporus*	2016	ulcerative colitis, pneumonia	45	dead
IFM 65030	*A. latus*	*A. spinulosporus*	2017	bronchiolitis	62	alive
IFM 65233	*A. latus*	*A. spinulosporus*	2018	liver cirrhosis, chronic pulmonary aspergillosis	66	alive
IFM 65329	*A. latus*	*A. spinulosporus*	2015	pulmonary non-tuberculous mycobacteriosis, chronic pulmonary aspergillosis	68	alive
IFM 66778	*A. latus*	*A. spinulosporus*	2020	acute myeloid leukemia, invasive pulmonary aspergillosis	13	alive

384

385

386 **Table 2.** Morphological comparison of *Aspergillus latus*, *A. spinulosporus* and *A. sublatus*.

		A. latus This study	*A. spinulosporus* This study & [35]	*A. sublatus* This study & [36]
Colony	CYA	Obverse: yellow green, olive green, pale brown edge	Obverse: pale brown, yellow edge, grey, green conidia forming all over	Obverse: reddish brown, grey, pale brown edge, reddish conidia forming in the center
		Reverse: dark brown, yellowish brown, green conidia formed in the center	Reverse: pale brow, brown,	Reverse: pale brown, orange, brown edge
	MEA	Obverse: pale yellow, irregular edge with white mycelia	Obverse: concentrically growth, pale-yellow	Obverse: concentrically growth, pale-yellow, white edge, olive-green conidia formed in the center
		Reverse: pale-yellow, soluble yellowish pigments present and exudates absent	Reverse: pale yellow, soluble pigments and exudates absent	Reverse: pale yellow, no soluble pigments and exudates
	OA	Obverse: pale brown, green, partially reddish, covered in green conidia, the center pigmented yellow to brown	Obverse: pale brown with olive green conidia and sometime wrinkled	Obverse: brown with pale brown edge
		Reverse: soluble orange or brown pigments present and exudates absent	Reverse: orange to brown, brown soluble pigments present and exudates absent	Reverse: orange to brown, brown soluble pigments present and exudates absent

Ascomata	character	cleistothecial, superficial, black, globose, subglobose, surrounded by Hülle cells	cleistothecial, superficial, dark brown, globose, subglobose, surrounded by Hülle cells	cleistothecial, superficial, red to purple, globose, subglobose
Hülle cells	size (µm)	8.7–20 (diameter)	14–30 (diameter)	12.5–30× 10–28
	character	hyaline, globose to ovoid	hyaline, globose to ovoid	hyaline, globose to ovoid
Ascospores	size (µm)	3.5–10 (pleated equatorial crests: 0.6–2.3)	3.5–4.5 × 3.0–4.5 (pleated equatorial crests: 0.8–1.0)	4.0–4.5 × 3.0–3.5 (pleated equatorial crests: 1.0–1.5)
	character	purple red, reddish brown, in surface view globose, subglobose, spore bodies smooth, incompletely reticulate, ribbed, globose, subglobose, in side view lenticular, with two pleated equatorial crests	orange,reddish brown, in surface view globose, subglobose, spore bodies echinulate, globose, subglobose, in side view lenticular	purple red, reddish brown, globose, subglobose, spore bodies smooth, in side view lenticular
Conidiophores	size (µm)	50–179 × 2.0–3.6	70–120 × 5.0–6.0	200× 4.0–6.0
	character	smooth stipes, pale brown	smooth stipes, yellowish brown	pale grey, grayish yellow
Vesicles	size (µm)	4.8–9.0 (wide)	9.0–11 (wide)	9.0–12.5 (wide)
	character	pale brown, subglobose to subclavate	yellowish brown, subclavate, fertile over the upper half	hemispherical, flask-shaped
Metulae	size (µm)	5.1–8.3 × 2.0–4.0	6.0–8.0 × 3.0–4.0	4.0–6.0 × 3.0–4.0
	character	hyaline to pale green	pale brown to pale green	hyaline to pale yellowish brown
Phialides	size (µm)	5.2–8.4 × 2.0–4.0	6.0–8.5 × 2.0–3.0	6.0–8.0 × 2.0–3.0
	character	hyaline, flask-shaped	hyaline to pale green, flask-shaped	hyaline to pale yellowish brown

Conidia	size (µm)	2.7–4.8	3.0–4.0	2.5–3.5(4.0)
	character	echinulate, globose to subglobose, green in mass	echinulate, globose to subglobose, green in mass	echinulate, globose to subglobose, green to pale olive green

387

388 **Table 3.** MIC values for antifungal drugs

Species name	Strain No.	MIC (μg/mL)					
		MCFG	CPFG	AMPH-B	ITCZ	VRCZ	MCZ
Aspergillus latus	IFM 61956	0.06	16	4	0.5	0.12	2
	IFM 63852	0.12	16	4	0.25	0.12	1
	IFM 64360	0.06	16	4	0.25	0.25	1
	IFM 65030	0.06	4	4	0.25	0.06	1
	IFM 65233	0.06	2	4	0.5	0.06	1
	IFM 65329	0.03	8	4	0.25	0.12	2
	IFM 66778	0.06	4	8	0.25	2	0.5
A. sublatus	IFM 42029^{T}	>16	16	4	0.25	0.12	2
A. spinulosporus	IFM 66771	0.15>	2	1	0.25	0.25	0.5
	IFM 61449	>16	8	0.5	0.25	0.12	0.5
	IFM 64750	>16	8	1	0.25	0.12	1

MCFG = micafungin, CPFG = caspofungin, AMPH-B = amphotericin B, ITCZ = itraconazole, VRCZ = voriconazole, MCZ = miconazole

389

390

391 **Figure legends**

392 **Fig. 1**. Phylogenetic tree constructed using maximum likelihood (ML) analysis based on the

393 models selected with the GTRCAT for *CaM* (Bootstrap value: > 70%). *A. aurantiobrunneus* and

394 *A. fructus* were used as outgroup. Numbers after taxa are isolate, specimen or strain numbers. The

395 scale bar represents the number of nucleotide substitutions per site. The sequences obtained in

396 this study are shown in bold. T = type sequence.

397

398 **Fig. 2**. *A. latus* IFM 65329 colonies: obverse CYA 37 °C (A), MEA 37 °C (B), OA 25 °C (C),

399 reverse: CYA 37 °C (D), MEA 37 °C (E), OA 25 °C, 7d (F), conidiophores (G–J), conidia (K),

400 Hülle cells (L), ascomata (M), ascospores (N, O) Scale bars: G–L, N, O 10 µm.

401

Shibata et al.
Figure 1

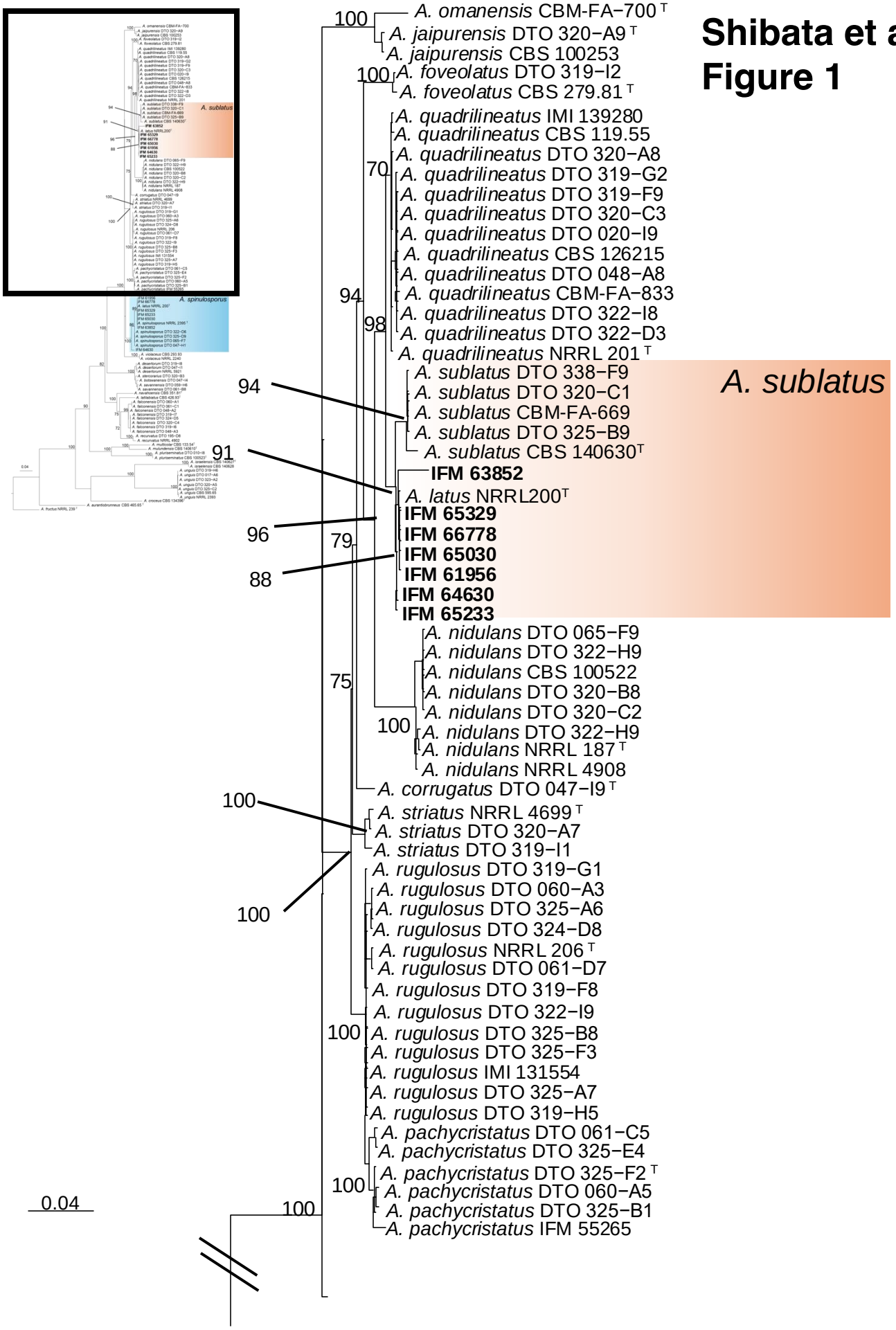

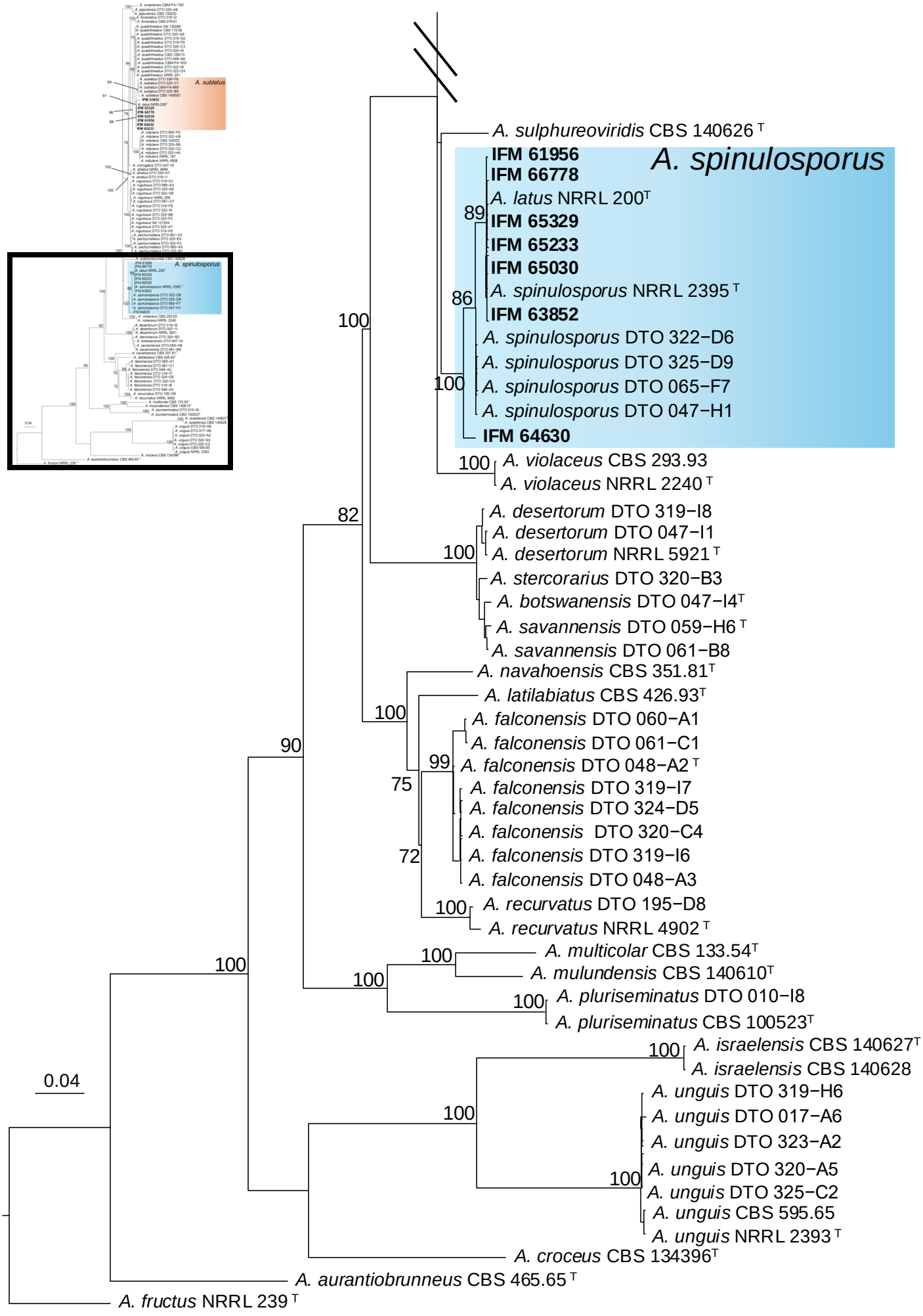
A. sublatus
A. spinulosporus
A. sulphureoviridis CBS 140626 T
IFM 61956
IFM 66778
A. latus NRRL 200T
IFM 65329
IFM 65233
IFM 65030
A. spinulosporus NRRL 2395 T
IFM 63852
A. spinulosporus DTO 322−D6
A. spinulosporus DTO 325−D9
A. spinulosporus DTO 065−F7
A. spinulosporus DTO 047−H1
IFM 64630
A. violaceus CBS 293.93
A. violaceus NRRL 2240 T
A. desertorum DTO 319−I8
A. desertorum DTO 047−I1
A. desertorum NRRL 5921 T
A. stercorarius DTO 320−B3
A. botswanensis DTO 047−I4T
A. savannensis DTO 059−H6 T
A. savannensis DTO 061−B8
A. navahoensis CBS 351.81T
A. latilabiatus CBS 426.93T
A. falconensis DTO 060−A1
A. falconensis DTO 061−C1
A. falconensis DTO 048−A2 T
A. falconensis DTO 319−I7
A. falconensis DTO 324−D5
A. falconensis DTO 320−C4
A. falconensis DTO 319−I6
A. falconensis DTO 048−A3
A. recurvatus DTO 195−D8
A. recurvatus NRRL 4902 T
A. multicolar CBS 133.54T
A. mulundensis CBS 140610T
A. pluriseminatus DTO 010−I8
A. pluriseminatus CBS 100523T
A. israelensis CBS 140627T
A. israelensis CBS 140628
A. unguis DTO 319−H6
A. unguis DTO 017−A6
A. unguis DTO 323−A2
A. unguis DTO 320−A5
A. unguis DTO 325−C2
A. unguis CBS 595.65
A. unguis NRRL 2393 T
A. croceus CBS 134396T
A. aurantiobrunneus CBS 465.65 T
A. fructus NRRL 239 T
0.04
100
89
86
100
100
82
100
90
100
75
99
72
100
100
100
100
100
100
100
100

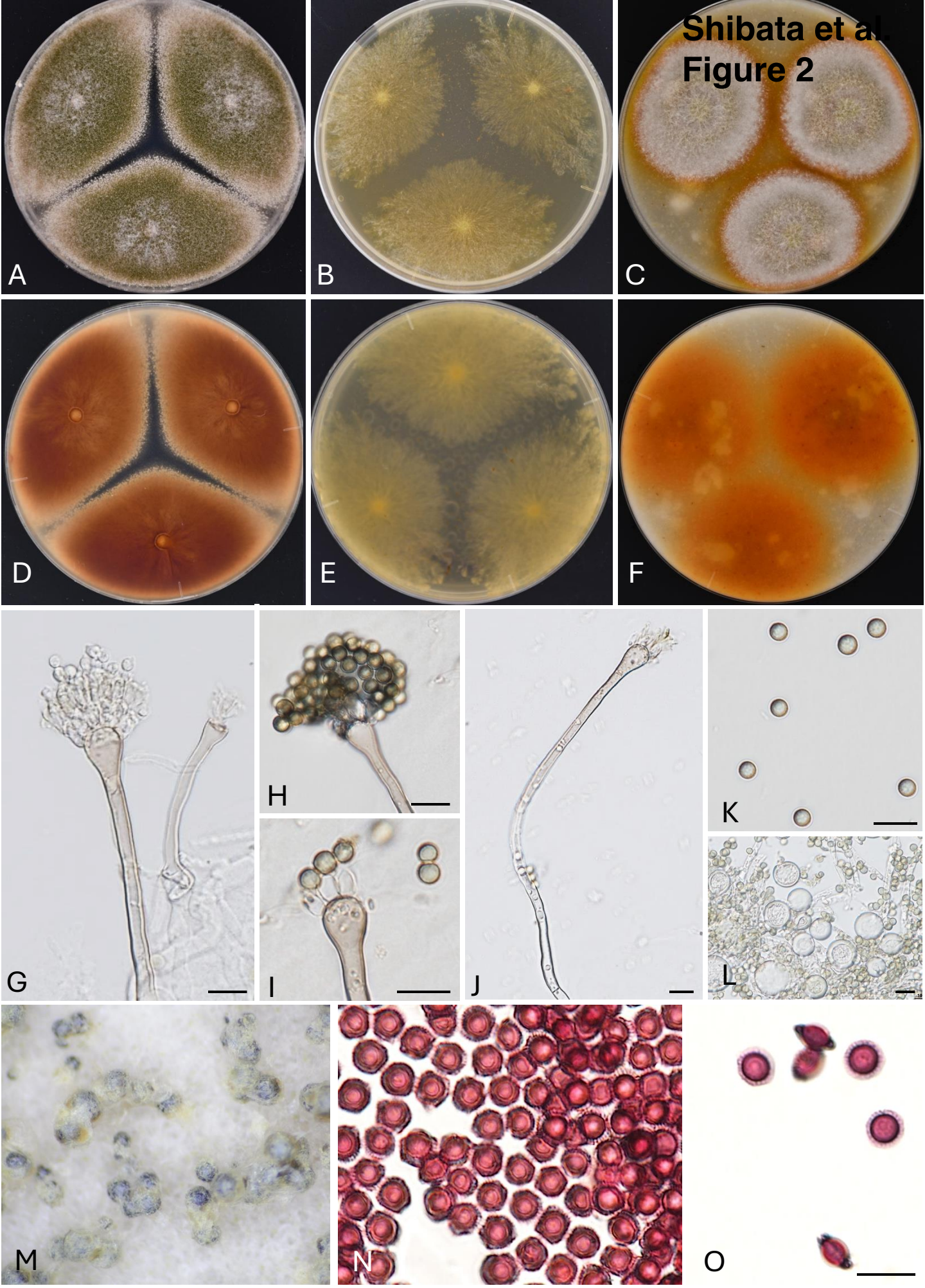
Shibata et al.
Figure 2
A
B
C
D
E
F
G
H
I
J
K
L
M
N
O